BIOINFORMATICS ORIGINAL PAPER Vol. 26 no. 22 2010, pages 2874–2880
doi:10.1093/bioinformatics/btq517

Systems biology

Advance Access publication September 8, 2010

Fixed point characterization of biological networks with complex graph topology

N. Radde

Institute for Systems Theory and Automatic Control, University of Stuttgart, Pfaffenwaldring 9, 70550 Stuttgart, Germany

Associate Editor: Martin Bishop

ABSTRACT

Motivation: Feedback circuits are important motifs in biological networks and part of virtually all regulation processes that are needed for a reliable functioning of the cell. Mathematically, feedback is connected to complex behavior of the systems, which is often related to bifurcations of fixed points. Therefore, several approaches for the investigation of fixed points in biological networks have been developed in recent years. Many of them assume the fixed point coordinates to be known, and an efficient way to calculate the entire set of fixed points for interrelated feedback structures is highly desirable.

Results: In this article, we consider regulatory network models, which are differential equations with an underlying directed graph that illustrates independencies among variables. We introduce the circuit-breaking algorithm (CBA), a method that constructs one-dimensional characteristics for these network models, which inherit important information about the system. In particular, fixed points are related to the zeros of these characteristics. The CBA operates on the graph topology, and results from graph theory are used in order to make calculations efficient. Our framework provides a general scheme for analyzing network models in terms of interrelated feedback circuits. The efficiency of the approach is demonstrated on a model for calcium oscillations based on experiments in hepatocytes, which consists of several interrelated feedback circuits.

Contact: radde@ist.uni-stuttgart.de

Supplementary information: Supplementary data are available at *Bioinformatics* online.

Received on July 14, 2010; revised on August 17, 2010; accepted on September 3, 2010

1 INTRODUCTION

Ordinary differential equations are used in essentially all scientific fields to describe dynamic behaviors of physical, biological or technical systems. An analysis of these systems usually starts with an investigation of their limit sets, in particular, the fixed points and their local phase portraits. In order to calculate the fixed points of a system $\dot{x}=f(x)$ with $x\in\mathbb{R}^n$, algorithms such as Newton's method and related approaches (Knoll and Keyes, 2004) are commonly used. Besides the well-known problems of those methods concerning convergence, they require the calculation of the Jacobian matrix in each step, which can in most cases only be done via numeric approximations. Consequently, these methods are often computationally expensive, especially if n is large. It is thus difficult to investigate, for example, the dependence of fixed point coordinates on model parameters, which requires calculating the fixed points for multiple parameter values.

In many applications the differential equation system describes the dynamics of interacting components, and a component is usually not influenced by all other components, but by a subset of these. These dependencies can be illustrated by a directed graph: if $\dot{x}_i$ is influenced by x_j, we indicate this with a directed edge from vertex v_j to vertex v_i in the graph, and the dynamics, in particular, the fixed point coordinates of x_i, depend on x_j. Thus, all fixed point coordinates of components in a circuit are dependent, and the idea of our approach is to exploit these dependencies in order to reduce the dimension of the fixed point equations $f(\bar{x})=0$.

The concept of our approach will be explained in the context of biological networks. More precisely, we consider intracellular regulation processes with underlying directed graph structure, such as gene regulatory networks (RNs). These systems are commonly based on chemical reaction kinetics, resulting in nonlinear models that cannot be solved analytically. Fixed points play an essential role in those models, since the emergence of complex behavior is often related to local bifurcations of those points. Bi- or multistability, which comes along with phenomena such as switching behavior, decision processes or memory effects, are generically caused by saddle-node bifurcations. Biological examples for these phenomena are numerous: switching mechanisms in multisite protein phosphorylation, which play a role in eukaryotic signaling cascades (Angeli *et al.*, 2004; Gunawardena, 2005), lysis or lysogenic pathway selection by phage λ-infected *Escherichia coli* cells (Arkin *et al.*, 1998 and references therein) cellular differentiation processes (Huang *et al.*, 2007) or epigenetic differences caused by transient signals such as the state of the lactose operon in *Escherichia coli* (Santillán and Mackey, 2008). Oscillations are generically created by Hopf bifurcations of fixed points (Chen and Aihara, 2002; Radde, 2009; Xiao and Cao, 2008) and all those behaviors have been related to circuits in the underlying interaction graphs (I-graphs) (Novák and Tyson, 2008; Radde *et al.*, 2010; Wagner, 2005).

Besides a calculation of fixed points for constructing bifurcation diagrams, investigating the fixed points of intracellular networks is also facilitated by experimental data, since in many settings only fixed point measurements under different perturbations are available, while kinetic data are missing (Steinke *et al.*, 2007). Along these lines, analysis methods which operate on the fixed points of these networks have been developed in recent years. Examples are robustness analysis with respect to kinetic perturbations, that is,

perturbations which leave the steady state fluxes invariant (Waldherr *et al.*, 2009), or sensitivity analysis locally about fixed points. All these methods require a calculation of the fixed points in advance.

In this article, we consider RN models, which are systems of differential equations with underlying I-graphs. Vertices in these graphs correspond to variables, and edges indicate any kind of regulation. We introduce the circuit-breaking algorithm (CBA), which constructs one-dimensional circuit characteristics whose zeros correspond to the fixed point values of RNs. The principal idea of our approach is to exploit the dependencies among fixed point coordinates of variables in a feedback circuit and to describe the set of fixed points with a minimal set of independent variables. We show that the cardinality of this set is related to the number of independent elementary circuits in the I-graph. Therefore, the circuits in the graph are broken, the fixed points of the acyclic system are analyzed, and characteristics are constructed by iteratively closing the circuits. The algorithm operates on the graph topology, and results from graph theory are used to optimize efficiency, which is mainly determined by the structure of interlinked circuits. Thus, our approach provides a connection between graph theory and dynamical systems theory and is applicable in a very general setting. The article is organized in the following manner: first, we introduce the modeling framework for RNs. Then the CBA for fixed point calculation in those models is explained. Finally, we show an application of the method to a RN model for calcium oscillations based on experiments in hepatocytes (Kummer *et al.*, 2000).

2 MODELING FRAMEWORK

We consider differential equation models for RNs of the form

$$\dot{x}_i(t) = f_i(x(t)) \quad i = 1,\dots,n \tag{1}$$

with state vector $x \in \mathbb{R}^n$ and continuously differentiable vector field $f : U \to \mathbb{R}^n \in \mathcal{C}^1$ defined on an open subset $U \subseteq \mathbb{R}^n$. The corresponding initial value problem with initial state $x(t=0) = x_0$ has a unique and smooth solution $\varphi(t, x_0)$ defined on an interval I_{x_0} (Guckenheimer and Holmes, 1990). System (1) should have a finite set of fixed points with at least one element, which is required later on to ensure termination of the algorithm. We consider this assumption not as a strong restriction. It is fulfilled for nearly all models based on chemical reaction kinetics. Since the existence of a compact and positively invariant set implies the existence of a fixed point inside, which is an extension of the Brouwer Fixed Point Theorem (Basener *et al.*, 2006), it is often sufficient to show that such a set exists.

We will work with the system's underlying network structure. More precisely, we consider the I-graph $G(V,E)$ with vertex set $V = \{v_1,\dots,v_n\}$ corresponding to the variables of the system and an edge set E defined in the following way:

$$e_{ii} \in E \;\Leftrightarrow\; \exists x \in U \text{ such that } \frac{\partial f_i}{\partial x_i} > 0 \tag{2}$$

$$e_{ij} \in E, i \neq j \;\Leftrightarrow\; \exists x \in U \text{ such that } \frac{\partial f_i}{\partial x_j} \neq 0 \tag{3}$$

The I-graph is a digraph that might contain loops in case of positive auto-regulations. This definition of a RN model is very general and includes as a special case models in which the partial derivatives $\partial f_i/\partial x_j$, $i \neq j$, have constant signs independent of the system's state or, equivalently, the off-diagonal elements in the Jacobian matrix of the system have constant sign structure. This is a well-investigated model class (Angeli *et al.*, 2010; Gouzé, 1998; Letellier and Vallée, 2003; Radde *et al.*, 2010; Thomas, 1981) with I-graphs that have sign-labeled edges. Signs of (semi)paths or (semi)circuits are defined within this class as the product of signs of edges belonging to the paths or circuits, respectively. They have been proven useful for the analysis of these models in many respects. However, since this monotonicity constraint is not always fulfilled in biological examples, we do not want to be too restrictive at this point and allow for sign changes and zeros of the partial derivatives as well. Thus, some edges in the I-graph might have sign-labels, others do not. This relaxation is a crucial extension to previous work, since many graph-theoretical considerations strongly rely on these monotonicity constraints (Angeli *et al.*, 2010; Gouzé, 1998). To conclude, a RN is defined here as a tuple $(\mathcal{D}, G)$ of a dynamical system $\mathcal{D}$ and an underlying digraph $G(V,E)$, called the I-graph, which is completely determined by $\mathcal{D}$. Edges of G might be labeled if the respective partial derivative has a constant sign independent of the system's state.

3 THE CBA

3.1 Idea

The idea of our approach is that fixed points of a circuit are completely characterized by knowing the fixed point coordinate of just one of the variables in the circuit. To illustrate the point, we consider the following single circuit system with n vertices:

$$\dot{x}_1(t) = f_1(x_1(t), x_n(t)) \tag{4}$$

$$\dot{x}_i(t) = f_i(x_i(t), x_{i-1}(t)) \;\; i = 2,\dots,n. \tag{5}$$

The procedure is shown in Figure 1 for three vertices. According to our definition of RNs, the diagonal elements of the Jacobian matrix are non-positive here (otherwise the system had loops). In order to calculate the fixed points of the system, in a first step we break the circuit by cutting the edge from vertex v_n to vertex v_1 and fixing variable x_1 to a value κ_1. The fixed point coordinates of this *directed acyclic graph* (DAG) can now be calculated as functions of κ_1. Here, the set $\bar{x}_2(\kappa_1)$ is implicitly given by

$$f_2(\bar{x}_2, x_1 = \kappa_1) = 0, \tag{6}$$

and we proceed iteratively for the remaining vertices, such that $\bar{x}_i(\kappa_1)$ is characterized by

$$f_i(\bar{x}_i, x_{i-1} = \bar{x}_{i-1}(\bar{x}_{i-2}(\dots(\kappa_1)))) = 0 \quad i = 3,\dots,n. \tag{7}$$

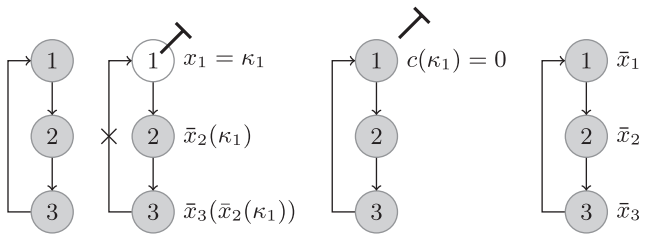

Fig. 1. Idea of the CBA illustrated with a single circuit: the circuit is broken by fixing variable $x_1 = \kappa_1$, and the set of fixed point coordinates of the acyclic system is iteratively calculated as a function of κ_1. Then the circuit is closed by constructing the circuit characteristic $c(\kappa_1)$, whose zeros are the fixed point coordinates $\bar{x}_1$. Finally, the set $\bar{x}_1$ is used as input to calculate the set $\bar{x}$ of fixed points of the system.

We keep in mind that this iterative calculation scheme for fixed point coordinates in dependence of the values of the parent vertices can be applied to any RNs with acyclic I-graphs. The circuit is closed by solving the equation

$$f_1(\kappa_1, x_n = \bar{x}_n(\kappa_1)) \stackrel{!}{=} 0, \tag{8}$$

leading to a set of solutions $\bar{x}_1$, which are the fixed point values of x_1. Subsequently, we will refer to $f_1(\kappa_1, \bar{x}_n(\kappa_1))$ as *circuit-characteristic* $c(\kappa_1)$ *associated with variable* x_1 and to solving Equation (8) as *circuit-closing step*, which is the important step in our algorithm. Solutions generally have to be calculated numerically. The input of the function f_1 is the value κ_1 and the set $\bar{x}_n(\kappa_1)$, which also might have to be calculated numerically. Since the sets $\bar{x}_i(\kappa_1)$, $i = 2, \ldots, n$, are uniquely determined by κ_1, we can also skip this second input in Equation (8), bearing in mind that $c(\kappa_1)$ does not necessarily describe a function of κ_1. The set $\bar{x}_n(\kappa_1)$ are the fixed point branches of a bifurcation diagram with κ_1 as bifurcation parameter and might be empty or contain several elements depending on the value of κ_1. Having determined the set $\bar{x}_1$, all other fixed point coordinates can again iteratively be calculated by inserting elements of this set into Equations (6) and (7), in the same order as before. Thus, the zeros of $c(\kappa_1)$ completely characterize the fixed points of the system.

A similar scheme for a single negative circuit oscillator model and analytically calculable set $\bar{x}_n$ was used in Pigolotti *et al.* (2007), which was not explicitly stated there. Note that we could as well have started by fixing another variable in the circuit, which would have led to a different characteristic, but we will see that some properties are completely determined by the graph topology and are independent of the chosen associated variable.

The idea of constructing a one-dimensional characteristic whose zeros correspond to the fixed points of an RN model by breaking the circuits in the I-graph can be generalized for RNs with arbitrary I-graph topology. In the following, we will set up the scheme for constructing such a characteristic given the I-graph $G(V, E)$, and we call this procedure the CBA. The main difference when going to more complex graph topologies is that the circuit characteristic cannot always be constructed in a single circuit-closing step. Generally, we have to do the procedure several times, depending on the I-graph topology. We will often make use of graph-theoretical algorithms for efficient calculations.

3.2 Generalization to strongly connected graphs

Given an RN $(\mathcal{D}, G)$ with strongly connected I-graph $G(V, E)$, the CBA proceeds as follows to construct a circuit characteristic and to calculate the set of fixed points of the system.

3.2.1 Find set C of elementary circuits We start by listing the elementary circuits in $G(V, E)$ in a set C of subsets of vertices. Elementary circuits are circuits in which each vertex is encountered only once while moving along the circuit. Several algorithms have been proposed for finding this set C (Szwarcfiter and Lauer, 1976; Tarjan, 1972, 1973; Tiernan, 1970), which can be done in $\mathcal{O}(|V| + |E|(|C| + 1))$ time, where $|V|$, $|E|$ and $|C|$ denote the number of vertices, edges and elementary circuits in G, respectively.

3.2.2 Determine minimal circuit-covering vertex set $\widetilde{V}$ Second, we determine a *minimal circuit-covering vertex set* $\widetilde{V}$ for C, that is, a minimal subset $\widetilde{V}$ of V such that each element in C contains at least one vertex in $\widetilde{V}$. We denote the number of elements in $\widetilde{V}$ by M. M is crucial for the efficiency of the algorithm, since it determines the minimal number of circuit-closing steps needed for the calculation of the fixed point set $\bar{x}$ of the system. Let the elements in $\widetilde{V}$ be $\widetilde{V} = \{v_{m_1}, \ldots, v_{m_M}\}$. The rest of the vertices is collected in the set $\widehat{V} = V \setminus \widetilde{V} = \{v_{l_1}, \ldots, v_{l_L}\}$ with $L + M = |V|$. Both sets are changed during the CBA: in each circuit-closing step, one element in $\widetilde{V}$ is shifted to $\widehat{V}$, and finally $\widetilde{V} = \emptyset$ and $\widehat{V} = V$.

PROPOSITION 1. Finding a minimal circuit-covering vertex set $\widetilde{V} \subseteq V$ in a digraph $G(V, E)$ is an non-deterministic polynomial-time (NP)-hard optimization problem.

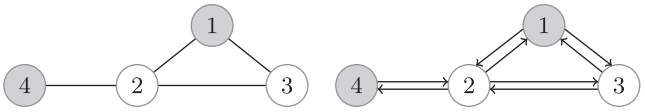

Fig. 2. Instances of the NP-hard VC problem on undirected graphs can be reformulated to finding a minimal circuit-covering vertex set $\widetilde{V}$ in a digraph by replacing each undirected edge with two edges of opposite direction. Here, the white vertices represent a VC in the undirected graph (left panel) and a minimal circuit-covering vertex set in the respective digraph (right panel).

PROOF. Instances of the *vertex cover* (VC) problem can be translated into finding a minimal circuit-covering vertex set $\widetilde{V}$. A VC of an undirected graph is a minimal subset $V^* \subseteq V$ of vertices such that each edge in the graph is incident to at least one vertex in V^*. Finding such a set V^* is an NP-hard optimization problem (Korte and Vygen, 2008). It is easy to verify that the problem of finding a VC in an undirected graph corresponds to finding a minimal circuit-covering vertex set $\widetilde{V}$ in the corresponding digraph, which is constructed by replacing all edges in the undirected graph by two edges of opposite direction. This is illustrated in Figure 2 by a graph with four vertices that has VC-number 2. The vertices marked in white are a VC in the undirected graph (Fig. 2, left panel), and at the same time also a minimal circuit-covering vertex set $\widetilde{V}$ in the respective digraph (Fig. 2, right panel). Note that if the I-graph had loops, the corresponding vertices can be included into the set $\widetilde{V}$ a priori, since they have to be contained in each minimal circuit-covering vertex set in any case, and the problem of finding $\widetilde{V}$ can be reduced by operating on the subgraph induced by the rest of the vertices. ■

3.2.3 Calculate the circuit-characteristic $c(\kappa_M)$ In the next step, we use the set $\widetilde{V}$ to determine a circuit-characteristic $c(\kappa_M)$ associated with variable x_{m_M}, which is afterwards used to calculate the fixed points $\bar{x}$ of the RN model. To this end, all circuits in G are broken by fixing the vertices in $\widetilde{V}$, i.e. setting $x_{m_j} =: \kappa_j, j = 1, \ldots, M$. For convenience, we summarize all κ_j in a single vector $\kappa \in \mathbb{R}^M$. This vector κ serves as input for the circuit-free system, and, since the acyclic I-graph has a topological order, the fixed point coordinates of the remaining vertices $\{v_{l_1}, \ldots, v_{l_L}\} \in \widehat{V}$ can iteratively be calculated as functions of the input κ. This translates to solving L equations

$$f_{l_p} : \mathbb{R} \times \mathbb{R}^{|\widetilde{V}|} \to \mathbb{R}, f_{l_p}(\bar{x}_{l_p}, \kappa) = 0 \quad p = 1, \ldots, L \tag{9}$$

for $\bar{x}_{l_p}$. The solutions of these L equations are collected in a set $\bar{x}_{\widehat{V}}(\kappa)$. In the next step, the circuits are closed one after another by releasing vertices in $\widetilde{V}$: for all $j = 1, \ldots, M$, we calculate the zeros of the *partial circuit-characteristics* $p_j(\kappa_j, \kappa)$, which is done by first reducing the set $\widetilde{V}$ by vertex v_{m_j} and the vector κ by component κ_j and then solving the implicit equation

$$f_{m_j} : \mathbb{R} \times \mathbb{R}^{|\widetilde{V}|} \to \mathbb{R}, f_{m_j}(x_{m_j} = \kappa_j, \bar{x}_{\widehat{V}}(\kappa, \kappa_j), \kappa) \stackrel{!}{=} 0 \tag{10}$$

for x_{m_j} to obtain a set $\bar{x}_{m_j}(\kappa)$ of fixed point coordinates for variable x_{m_j} in dependence of the values κ of vertices in the set $\widetilde{V}$. Thereby circuits containing x_{m_j} are closed. Similar to Equation (8), for fixed κ, the set $\bar{x}_{\widehat{V}}(\kappa, \kappa_j)$ describes fixed point branches of a bifurcation diagram with bifurcation parameter κ_j. Having determined the solution set $\bar{x}_{m_j}(\kappa)$, vertex v_{m_j} is shifted to $\widehat{V}$. The cardinality of the set $\widetilde{V}$, which determines the dimension of the respective partial circuit characteristic, is reduced by one in each circuit-closing step, such that we finally end up with a one-dimensional circuit characteristic

$$p_M =: c(\kappa_M) : \mathbb{R} \to \mathbb{R}, f_{m_M}(x_{m_M} = \kappa_M, \bar{x}_{\widehat{V}}(\kappa_M)) \tag{11}$$

associated with variable x_{m_M}.

3.2.4 Calculate set of fixed points $\bar{x}$ of the system The set of zeros of $c(\kappa_M)$ are the fixed point values $\bar{x}_{m_M}$ of vertex v_{m_M}. These can iteratively be inserted backwards into the partial circuit characteristics p_j, $j = M - 1, \ldots, 1$ in order

to obtain the fixed point coordinates of the other variables in the original set $\widetilde{V}$. Respective fixed point coordinates of the vertices that have originally been in $\widehat{V}$ can be calculated as well by inserting those values into $\bar{x}_{\widehat{V}}(\kappa)$, such that we have reconstructed the set $\bar{x}$ of zeros from the characteristic $c(\kappa_M)$.

The I-graph and signs of circuits contain information about the circuit-characteristic independent of the associated variable.

PROPOSITION 2. If only negative circuits of a strongly connected graph G are closed by releasing vertex v_{m_j}, the corresponding partial circuit characteristic $p_j(\kappa_j,\kappa)$ is strictly decreasing with respect to κ_j.

PROOF. We consider the derivative of the partial circuit characteristic

$$p_j(\kappa_j,\kappa):\mathbb{R}\times\mathbb{R}^{|\widetilde{V}|}\to\mathbb{R},f_{m_j}(x_{m_j}=\kappa_j,\bar{x}_{\widehat{V}}(\kappa,\kappa_j),\kappa) \tag{12}$$

with respect to κ_j for arbitrary $\kappa=\kappa^*$:

$$\frac{dp_j(\kappa_j,\kappa)}{d\kappa_j}\Big|_{\kappa^*}=\sum_{p,v_{l_p}\in\widehat{V}}\frac{\partial p_j}{\partial\bar{x}_{l_p}}\frac{d\bar{x}_{l_p}}{d\kappa_j}\Big|_{\kappa^*}+\frac{\partial p_j}{\partial\kappa_j}\Big|_{\kappa^*} \tag{13}$$

The last term is non-positive from the definition of the I-graph, which would have a positive loop otherwise, contrary to the assumption. Moreover, all terms in the sum are negative: The partial derivative is positive if the respective regulator v_{l_p} is an activator of the released vertex v_{m_j}, but in this case the path from v_{m_j} to v_{l_p} must be negative for the circuit to be negative, which translates into a negative derivative $\mathrm{d}\bar{x}_{l_p}/\mathrm{d}\kappa_j$. Contrary, if v_{l_p} is an inhibitor of v_{m_j}, the partial derivative is negative, but then the path from v_{m_j} to v_{l_p} must be positive, such that the product is again negative. Consequently, all terms in the derivative are negative. ■

It follows immediately that systems lacking positive circuits have at most one isolated fixed point, which was also proven in a different way by Gouzé (1998) and Snoussi (1998).

3.3 Generalization to arbitrary graph topologies

The CBA can be extended to RNs $(\mathcal{D},G)$ with I-graph $G(V,E)$ that is not strongly connected. Without loss of generality, we still assume connectedness of the graph. We have to consider the fixed point coordinates separately for each strongly connected component (SCC). In order to construct the set $\bar{x}$ from the individual fixed point sets of each component, we introduce the concept of *fixed point paths*.

3.3.1 Find SCCs In the first step, we partition the vertex set V into subsets $V=\{V^1,\ldots,V^K\}$ such that the subgraphs G^k induced by V^k are the SCC of G. This can be done in $\mathcal{O}(|V|+|E|)$ time by a depth first search algorithm as originally described by Tarjan (1972) (for a more recent improved algorithm see also Korte and Vygen, 2008). Contracting the vertices of SCCs yields a DAG, which has a topological order. Therefore, the fixed point coordinates can be calculated iteratively for each SCC, starting with the component on top of the hierarchy. When doing so, the fixed points $\bar{x}^k$ of a component k serve as constant inputs for calculating the fixed point coordinates of subsequent components. We assume that the subgraphs G^k are already hierarchically ordered, with G^1 being on top. Then we proceed by iteratively calculating the fixed point coordinates of each subgraph in the way explained before. This has to be done for each possible input, that is, for each fixed point set $\bar{x}^z$, $z=1,\ldots,k-1$ of the previous SCCs.

3.3.2 Determine fixed point paths Having calculated $\bar{x}^k$ for all k, these define the fixed point set $\bar{x}$ of the system. The following example illustrates how to achieve the set $\bar{x}$ of fixed points of the system from the sets $\bar{x}^k$:

$$\begin{aligned}\dot{x}_1 &= x_1(x_1-1)\\ \dot{x}_2 &= x_2(x_1x_2-1)\\ \dot{x}_3 &= e^{-x_3}-x_2\end{aligned} \tag{14}$$

The I-graph of the system and its SCCs with respective circuit sets and minimal circuit-covering vertex sets are shown in Figure 3. The fixed point

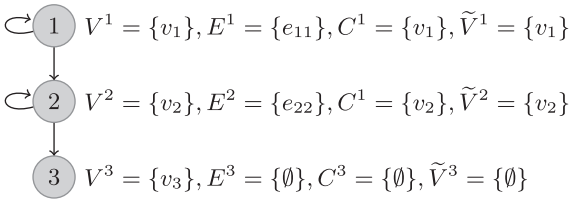

Fig. 3. I-graph, SCCs, circuit sets and minimal circuit-covering vertex sets of system (14).

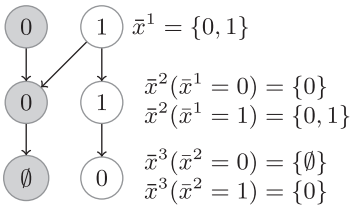

Fig. 4. Fixed point graph of system (14), which illustrates the interdependencies between the sets of fixed point values $\bar{x}^1,\bar{x}^2$ and $\bar{x}^3$. The paths not ending with an empty set define the fixed points of the system, here given by $\bar{x}=(1,1,0)$.

graph is illustrated in Figure 4. It is a DAG whose nodes correspond to the fixed point coordinates of the SCCs. *Fixed point paths* are the paths in this graph which do not end with an empty set. Here the only path is $(1,1,0)$, and the system has one fixed point $\bar{x}=(1,1,0)$.

4 APPLICATION OF THE CBA TO A MODEL FOR CALCIUM OSCILLATIONS

We illustrate the CBA on a network model for cytoplasmic calcium oscillations based on experiments in hepatocytes, which is described in Kummer *et al.* (2000):

$$\begin{aligned}\dot{x}_1 &= k_1+k_2x_1-k_3x_2\mathrm{m}(x_1,\theta_1)-k_4x_3\mathrm{m}(x_1,\theta_2)\\ \dot{x}_2 &= k_5x_1-k_6\mathrm{m}(x_2,\theta_3)\\ \dot{x}_3 &= k_7x_2x_3\mathrm{m}(x_4,\theta_4)+k_8x_2+k_9x_1-\\ &\quad k_{10}\mathrm{m}(x_3,\theta_5)-k_{11}\mathrm{m}(x_3,\theta_6)\\ \dot{x}_4 &= -k_7x_2x_3\mathrm{m}(x_4,\theta_4)+k_{11}\mathrm{m}(x_3,\theta_6)\end{aligned} \tag{15}$$

with $x=(\mathrm{Ga}^*,\mathrm{PLC}^*,\mathrm{Ca}_{cyt},\mathrm{Ca}_{er})$ denoting concentrations of an active G-protein-linked receptor, active phospholipase C enzyme, free calcium in the cytoplasm and calcium in the endoplasmic reticulum, respectively. The functions $\mathrm{m}(x,\theta)=x/(x+\theta)$ are Michaelis–Menten terms, and all rate constants k and Michaelis constants θ are non-negative. The model can show periodic oscillations and bursting. We are interested in the fixed points of the system in the positive orthant for parameter values given by $k_1=0.09,k_2=2,k_3=1.27,k_4=3.73,k_5=1.27,k_6=32.24,k_7=2,k_8=0.05,k_9=13.58,k_{10}=153,k_{11}=4.85,\theta_1=0.19,\theta_2=0.73,\theta_3=29.09,\theta_4=2.67,\theta_5=0.16,\theta_6=0.05$ (Peifer and Timmer, 2007). Since the positive orthant $\mathbb{R}^4_+$ is invariant for the flow, as can easily be seen by showing $\dot{x}_i(x_i=0)\geq 0$ for $i=1,\ldots,4$, we set $U=\mathbb{R}^4_+$. The vector field is continuously differentiable in this region. We note that U is not a trapping region for all initial

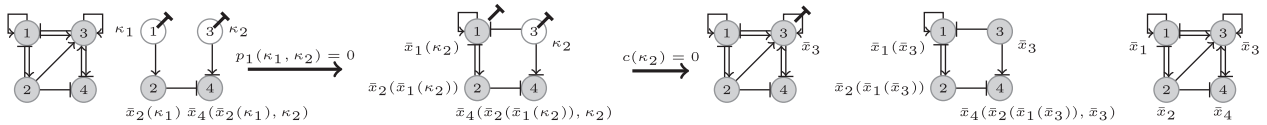

Fig. 5. The CBA applied to the calcium oscillation network described in Kummer *et al.* (2000). A minimal circuit-covering vertex set is given by $\widetilde{V}=\{1,3\}$. In the first step the circuits are broken by fixing all variables in $\widetilde{V}$, and the set of fixed point coordinates $\bar{x}_2$ and $\bar{x}_4$ are calculated as functions of the input $\kappa=(\kappa_1,\kappa_2)$. Then the circuits are iteratively closed, here by first releasing variable x_1. Mathematically, this translates into calculating the zeros $\bar{x}_1(\kappa_2)$ of the partial circuit characteristic $p_1(\kappa_1,\kappa_2)$. The final circuit characteristic, which is constructed by releasing vertex v_3, is a function of κ_2, and its zeros determine the set of fixed point coordinates $\bar{x}_3$. The fixed point coordinates of the other variables can be calculated by inserting elements of $\bar{x}_3$ into $\bar{x}_1(\kappa_2)$, leading to the set $\bar{x}_1$, and then into $\bar{x}_2(\bar{x}_1)$ and $\bar{x}_4(\bar{x}_1,\bar{x}_3)$.

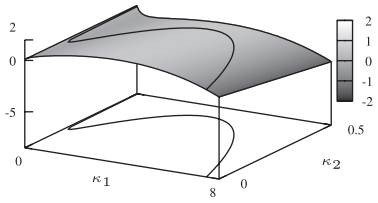

Fig. 6. Partial circuit characteristic $p_1(\kappa_1,\kappa_2)$ of the calcium oscillation network (15) along with the solution set $\bar{x}_1(\kappa_2)$ of $p_1(\kappa_1,\kappa_2)=0$.

conditions $x_0\in\mathbb{R}^n$, a property that can also be recognized by our characteristics.

The I-graph of this system (Fig. 5) is strongly connected, i.e. $K=1$, and we skip the index k here. All edges except e_{43} are sign labeled, which is indicated by arrows (activation) and blunt ends (inhibition). The circuit set consists of seven elements including three positive, three negative and one unsigned circuit, $C=\{\{1,2,3,4\},\{1\},\{3\},\{1,2\},\{1,3\},\{3,4\},\{1,2,3\}\}$. Since G contains positive and negative circuits, only from the topology neither multiple fixed points nor periodic behavior can be excluded a priori. A minimal circuit-covering vertex set is $\widetilde{V}=\{1,3\}$, and we identify $M=2$, $m_1=1$ and $m_M=3$. Vertices in the set $\widetilde{V}$ are marked in white in Figure 5. First, we break the circuits by setting $x_1=:\kappa_1$ and $x_3=:\kappa_2$, and calculate the fixed point values of variables in the set $\widehat{V}$, here x_2 and x_4, as functions of the input vector $\kappa\in\mathbb{R}^2$. This can be done analytically, and we obtain

$$f_2(\kappa,x_2)=0 \Leftrightarrow \bar{x}_2(\kappa)=\frac{k_5\kappa_1\theta_3}{k_6-k_5\kappa_1}$$

$$f_4(\kappa,x_4)=0 \Leftrightarrow \bar{x}_4(\kappa)=\frac{k_{11}\mathrm{m}(\kappa_2,\theta_6)\theta_4}{k_7\bar{x}_2(\kappa_1)\kappa_2-k_{11}\mathrm{m}(\kappa_2,\theta_6)}.$$

The first set of circuits is closed by releasing vertex v_1. We note that the subgraph induced by v_1 and v_2 has the structure of an activator-inhibitor oscillator model (Tyson, 2005) with input κ_2, a typical structure which is capable of producing oscillations and bistability (Chen and Aihara, 2002; Radde, 2009; Tyson, 2005). Mathematically, we reduce $\widetilde{V}$ by v_1 and κ by κ_1, such that $\widetilde{V}=\{v_3\}$ and $\kappa=\{\kappa_2\}$, and calculate the zeros $\bar{x}_1(\kappa_2)$ of the partial circuit characteristic

$$p_1(\kappa_1,\kappa):\mathbb{R}\times\mathbb{R}\to\mathbb{R},f_1(\kappa_1,\bar{x}_2(\kappa_1),\bar{x}_4(\kappa_1,\kappa_2),\kappa_2), \qquad (16)$$

here given by

$$k_1+k_2\kappa_1-k_3\bar{x}_2(\kappa_1)\mathrm{m}(\kappa_1,\theta_1)-k_4\kappa_2\mathrm{m}(\kappa_1,\theta_1). \qquad (17)$$

Having solved this equation, v_1 is shifted to $\widehat{V}$. The characteristic p_1 is shown in Figure 6, along with the contour $p_1=0$, which defines the solution set $\bar{x}_1(\kappa_2)$ that is used as input for the final circuit characteristic.

The sets $\bar{x}_1(\kappa_2)$,$\bar{x}_2(\kappa_2)$ and $\bar{x}_4(\kappa_2)$ are shown in Figure 7 (left panel, 1–3 figures from top). These graphs are bifurcation diagrams with κ_2 as a bifurcation parameter. The graph $\bar{x}_1(\kappa_2)$ shows that the subsystem consisting of the vertices v_1 and v_2 has a bistable range due to the positive auto-regulation of v_1 for $\kappa_2\in[0.18,0.42]$, with a lower stable fixed point $\bar{x}_1\approx 0$ (red line) and an upper one between 4 and 8 (blue line). These are separated by an unstable fixed point branch (green line). Since x_1 activates x_2, $\bar{x}_2(\kappa_2)$ has qualitatively the same course. The graph $\bar{x}_4(\kappa_2)$ shows several peculiarities of the x_4-dynamics: given κ_2, x_4 is produced with a constant synthesis rate $s=k_{11}\mathrm{m}(\kappa_2,\theta_6)$ and is degraded with a rate $\gamma=k_7\bar{x}_2(\kappa_2)\kappa_2\mathrm{m}(x_4,\theta_4)$ that has an upper bound $k_7\bar{x}_2(\kappa_2)\kappa_2$ independent of x_4. The bifurcation diagram $\bar{x}_4(\kappa_2)$ has poles at $s=\gamma$ (here two), and takes positive values only between these, which correspond to the upper stable fixed point branches of $\bar{x}_1$ and $\bar{x}_2$ (blue lines). This restricts first of all the range of possible values $\bar{x}_3$ to the range of values where positive solutions $\bar{x}_4>0$ exist, and second, it also shows that the positive auto-regulation of x_1 does not lead to two distinct stable steady states in the positive orthant for the complete system, since there are no positive solutions $\bar{x}_4$ for the lower stable fixed point branch $\bar{x}_1$.

For constructing the final circuit characteristic $c(\kappa_2)$ associated with variable x_3, we release vertex v_3, leading to

$$c(\kappa_2):=f_3(\bar{x}_2(\bar{x}_1(\kappa_2)),\kappa_2,\bar{x}_4(\kappa_2,\bar{x}_2(\bar{x}_1(\kappa_2))),\bar{x}_1(\kappa_2))=0 \qquad (18)$$

with

$$\bar{x}_4(\kappa_2,\bar{x}_2(\bar{x}_1(\kappa_2)))=\frac{k_{11}\mathrm{m}(\kappa_2,\theta_6)\theta_4}{k_7\bar{x}_2(\bar{x}_1(\kappa_2))\kappa_2-k_{11}\mathrm{m}(\kappa_2,\theta_6)}. \qquad (19)$$

The characteristic $c(\kappa_2)$ is shown in Figure 7 (bottom left panel). Most importantly, it has one zero at $\bar{x}_3=0.215$, and consequently the system has one fixed point, $\bar{x}=(6.43,9.9,0.215,34)$[1], which is calculated by inserting $\kappa_2=\bar{x}_3$ into $\bar{x}_i(\kappa_2)$, $i=1,2,4$. Graphically, this translates into simply reading off the respective values in the graphs $\bar{x}_i(\kappa_2)$ in Figure 7, indicated by the blue dashed line here.

Moreover, the characteristic indicates that the system might have the potential to show bistability for certain parameter values, since by shifting the curve to the positive y-direction, it eventually has three fixed points. We verified this by introducing a basic synthesis rate $s_3=95$ for x_3, which causes the desired shift of the characteristic. The value was read from the graph $c(\kappa_2)$.

[1]Precision is chosen according to the numeric values in the data files.

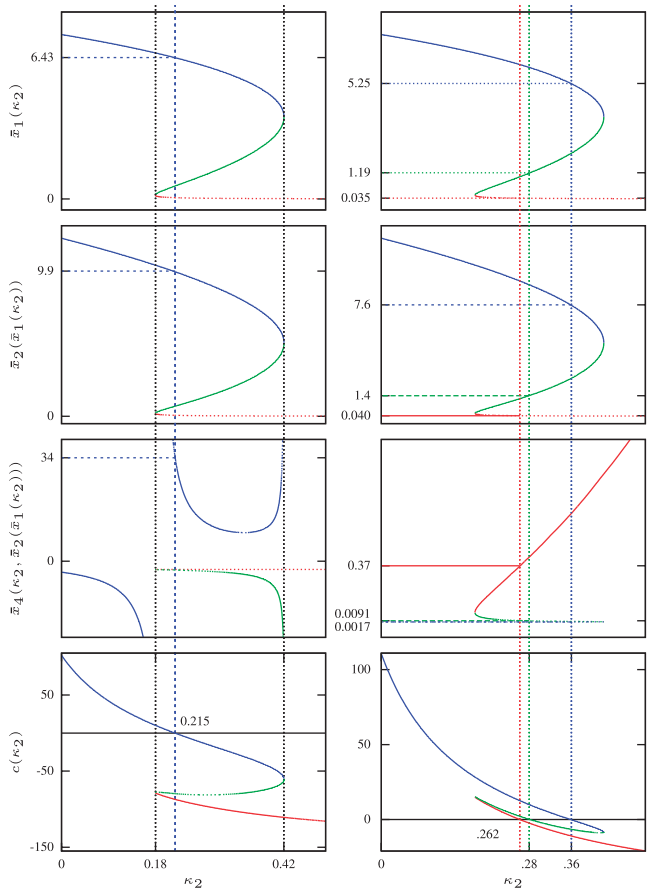

Fig. 7. From top to bottom: fixed point sets $\bar{x}_1(\kappa_2)$, $\bar{x}_2(\kappa_2)$ and $\bar{x}_4(\kappa_2)$, and circuit-characteristic $c(\kappa_2)$ associated with variable x_3 for the original (left panel) and modified (right panel) parameters as described in the text.

Moreover, we strengthened the positive auto-regulation term of x_3 by increasing k_7 to a value $k_7^*=20$ and slowed down x_3-degradation by setting $k_{11}^*=1$ and $\theta_6^*=10$. An additional decrease of the indirect negative circuit involving x_1 and x_3 by setting $k_9^*=2$ further enhanced the desired effect. Figure 7 (right panel) shows the respective characteristics. The sets $\bar{x}_1(\kappa_2)$ and $\bar{x}_2(\kappa_2)$ are both not affected by these parameter changes, and only $\bar{x}_4(\kappa_2)$ and $c(\kappa_2)$ are modified. The revised system has three fixed points in the positive orthant given by $\bar{x}^1 \approx (0.035, 0.040, 0.262, 0.37)$, $\bar{x}^2 \approx (1.19, 1.4, 0.28, 0.0091)$ and $\bar{x}^3 \approx (5.25, 7.6, 0.36, 0.0017)$[1]. Equations (17) and (18) were solved numerically using the latest version (4.4.0) of the open source plotting program gnuplot. Respective gnuplot files are available as Supplementary Material in pdf format. These are named 'barx' and 'barx2' for Figures 6 and 7 (left panel) and Figure 7 (right panel), respectively.[2]

[2]Before plotting, the files 'test1.dat' and 'test1b.dat' that are created by these programs were sorted, and line breaks between different branches were inserted manually. The formatted files are also available as Supplementary Material in rtf format.

5 CONCLUSION

This article considers RN models, which are described as systems of ordinary differential equations with an underlying directed graph structure, the I-graph. We have introduced the CBA for the characterization of fixed points of these models. The CBA exploits the dependencies of the fixed point coordinates in a connected graph in order to find a minimal characterization. Based on this idea, we constructed a one-dimensional circuit characteristic by breaking all circuits in the graph and iteratively closing them again. These circuit-closing steps correspond to solving implicit equations, whose dimensions are related to the circuit-structure of the graph. We demonstrated that this dimension is bounded from below by the cardinality of a minimal subset of vertices that covers the elementary circuits and explained how to construct the fixed point set of the system from the zeros of this circuit characteristic. Our approach has several advantages over purely numerical methods: first, in comparison to solving an n-dimensional equation $f(x)=0, x\in\mathbb{R}^n$, the dimension of the equations in the CBA can be much smaller, especially for sparse graphs. Second, we have demonstrated on a biological network model of interlocked feedback circuits that the influence of parameter variations on the fixed points can also be investigated by our algorithm. Thus, the constructed characteristics are, for example, useful to find bifurcations and parameter regions in which the system has a certain number of fixed points.

In this article, we applied the CBA to a network of four components. It can also be used to investigate fixed points of larger networks. The efficiency and superiority to Newton-type methods depend on the graph topology and increase when the cardinality of the minimal circuit-covering vertex sets decrease. We expect this to correlate with the sparsity of the graph, but it is not yet clear how we can further characterize the topology and behavior of such graphs. For larger networks, we expect that the computation of the SCCs, their circuit sets and especially the minimal circuit-covering vertex sets, is not negligible any more and increases the running time. We believe that our approach can especially facilitate the analysis of fixed point sets of smaller network models, and their dependence on parameter values. If the network consists of several interrelated feedback structures, it is in practice applicable to models of only few (say <10) components.

Finally, our approach is based on a very general framework and can be applied to a large class of differential equations. Complex dynamic behavior is related to circuits in the I-graphs, and the CBA provides an analysis method in terms of subnetworks with interrelated circuit structure. While in the past methodology has been developed for single feedback circuits, only few approaches exist that can handle complex feedback, and our method is a contribution in this direction. Recent studies indicate that complex network structures are often related to functional robustness, and methods to analyze these networks are thus highly relevant also from a biological point of view.

Several interesting question will guide our future work, most importantly, we believe that the circuit characteristics contain information about asymptotic properties of the system such as stability of the fixed points.

Funding: German Research Foundation (DFG) within the Cluster of Excellence in Simulation Technology (EXC 310/1) at the University of Stuttgart.

Conflict of Interest: none declared.

REFERENCES

Angeli,D. *et al*. (2004) Detection of multistability, bifurcations, and hysteresis in a large class of biological positive-feedback systems. *Proc. Natl Acad. Sci. USA*, **101**, 1822–1827.

Angeli,D. *et al*. (2010) Graph-theoretic characterizations of monotonicity of chemical reaction networks in reaction coordinates. *J. Math. Biol.*, **61**, 581–616.

Arkin,A. *et al*. (1998) Stochastic kinetic analysis of developmental pathway bifurcation in phage λ-infected *Escherichia coli* cells. *Genetics*, **149**, 1633–1648.

Basener,W. *et al*. (2006) The Brouwer Fixed Point Theorem applied to rumour transmission. *Appl. Math. Lett.*, **19**, 841–842.

Chen,L. and Aihara,K. (2002) A model of periodic oscillation for genetic regulatory systems. *IEEE Trans. Circuits Syst. I-Regul. Pap.*, **49**, 1429–1436.

Gouzé,J.-L. (1998) Positive and negative circuits in dynamical systems. *J. Biol. Syst.*, **6**, 11–15.

Guckenheimer,J. and Holmes,P. (1990) *Nonlinear oscillations, dynamical systems, and bifurcations of vector fields*. Number 42 in *Applied Mathematical Sciences*, Springer, New York.

Gunawardena,J. (2005) Multisite protein phosphorylation makes a good threshold but can be a poor switch. *Proc. Natl Acad. Sci. USA*, **102**, 14617–14622.

Huang,S. *et al*. (2007) Bifurcation dynamics in lineage-commitment in bipotent progenitor cells. *Dev. Biol.*, **305**, 695–713.

Knoll,D. and Keyes,D. (2004) Jacobian-free Newton-Krylov methods: a survey of approaches and applications. *J. Comput. Phys.*, **193**, 357–397.

Korte,B. and Vygen,J. (2008) *Combinatorial Optimization: Theory and Algorithms*. 4th edn. Springer, Berlin.

Kummer,U. *et al*. (2000) Switching from simple to complex oscillations in calcium signaling. *Biophys. J.*, **79**, 1188–1195.

Letellier,C. and Vallée,O. (2003) Analytical results and feedback circuit analysis for simple chaotic flows. *J. Phys. A Math. Gen.*, **36**, 11229–11245.

Novák,B. and Tyson,J. (2008) Design principles of biochemical oscillators. *Nat. Rev. Mol. Cell Biol.*, **9**, 981–991.

Peifer,M. and Timmer,J. (2007) Parameter estimation in ordinary differential equations for biochemical processes using the method of multiple shooting. *IET Syst. Biol.*, **1**, 78–88.

Pigolotti,S. *et al*. (2007) Oscillation patterns in negative feedback loops. *Proc. Natl Acad. Sci. USA*, **104**, 6533–6537.

Radde,N. *et al*. (2010) Graphical methods for analysing feedback in biological networks - a survey. *Int. J. Syst. Sci.*, **41**, 35–46.

Radde,N. (2009) The impact of time-delays on the robustness of biological oscillators and the effect of bifurcations on the inverse problem. *Eurasip J. Bioinf. Syst. Biol.*, **2009**, 14.

Santillán,M. and Mackey,M. (2008) Quantitative approaches to the study of bistability in the *lac* operon of *Escherichia coli*. *J. R. Soc. Interface*, **5**, S29–S39.

Snoussi,E. (1998) Necessary conditions for multistationarity and stable periodicity. *J. Biol. Syst.*, **6**, 3–9.

Steinke,F. *et al*. (2007) Experimental design for efficient identification of gene regulatory networks using sparse Bayesian models. *BMC Syst. Biol.*, **1**, 51.

Szwarcfiter,J. and Lauer,P. (1976) A search strategy for the elementary cycles of a directed graph. *Bit*, **16**, 192–204.

Tarjan,R. (1972) Depth-first search and linear graph algorithms. *SIAM J. Comput.*, **1**, 146–160.

Tarjan,R. (1973) Enumeration of the elementary circuits of a directed graph. *SIAM J. Comput.*, **3**, 211–216.

Thomas,R. (1981) On the relation between the logical structure of systems and their ability to generate multiple steady states or sustained oscillations. In Della-Dora,J. *et al*. eds, *Numerical Methods in the Study of Critical Phenomena*, Vol. 9 of *Springer Series in Synergetics*, Springer, New York, pp. 180–193.

Tiernan,J. (1970) An efficient search algorithm to find the elementary circuits of a graph. *Comm ACM*, **13**, 722–726.

Tyson,J. (2005) Biochemical oscillations. In Fall,C. *et al*. eds, *Computational Cell Biology*, Vol. 20 of *Interdisciplinary Applied Mathematics*, Springer, pp. 230–260.

Wagner,A. (2005) Circuit topology and the evolution of robustness in two-gene circadian oscillators. *Proc. Natl Acad. Sci. USA*, **102**, 11775–11780.

Waldherr,S. *et al*. (2009) Kinetic perturbations as robustness analysis tool for reaction networks. In *Proceedings of the 48th IEEE Conference on Decision and Control*, Shangai, China, pp. 4572–4577.

Xiao,M. and Cao,J. (2008) Genetic oscillation deduced from Hopf bifurcation in a genetic regulatory network with delays. *Math. Biosci.*, **215**, 55–63.